

Fluorescence “Turn On” Detection of Mercuric Ion Based on Bis(dithiocarbamato)copper(II) Complex Functionalized Carbon Nanodots

Chao Yuan,[†] Bianhua Liu,^{*,†} Fei Liu,[‡] Ming-Yong Han,[§] and Zhongping Zhang^{*,†}

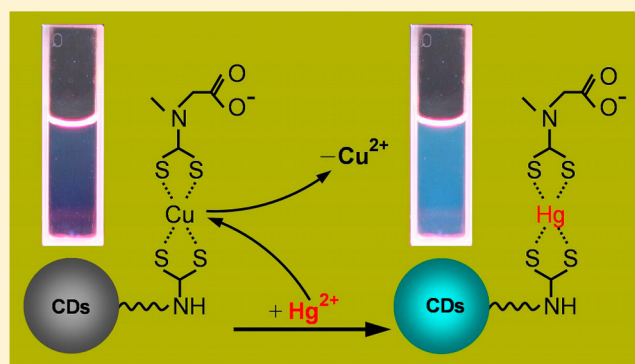
[†]Institute of Intelligent Machines, Chinese Academy of Sciences, Hefei, Anhui 230031, China

[‡]Fujian Inspection and Research Institute for Product Quality, Fuzhou, Fujian 350002, China

[§]Institute of Materials Research and Engineering, A-STAR, Research Link, 117602, Singapore

Supporting Information

ABSTRACT: A new “turn on” fluorescence nanosensor for selective Hg^{2+} determination is reported based on bis-(dithiocarbamato)copper(II) functionalized carbon nanodots ($\text{CuDTC}_2\text{-CDs}$). The CuDTC_2 complex was conjugated to the prepared amine-coated CDs by the condensation of carbon disulfide onto the nitrogen atoms in the surface amine groups, followed by the coordination of copper(II) to the resulting dithiocarbamate groups (DTC) and finally by the additional coordination of ammonium N-(dithiocarbonyl) sarcosine (DTCS) to form the CuDTC_2 -complexing CDs. The CuDTC_2 complex at surface strongly quenched the bright-blue fluorescence of the CDs by a combination of electron transfer and energy transfer mechanism. Hg^{2+} could immediately switch on the fluorescence of the $\text{CuDTC}_2\text{-CDs}$ by promptly displacing the Cu^{2+} in the CuDTC_2 complex and thus shutting down the energy transfer pathway, in which the sensitive limit for Hg^{2+} as low as 4 ppb was reached. Moreover, a paper-based sensor has been fabricated by printing the $\text{CuDTC}_2\text{-CDs}$ probe ink on a piece of cellulose acetate paper using a commercial inkjet printer. The fluorescence “turn on” on the paper provided the most conveniently visual detection of aqueous Hg^{2+} ions by the observation with naked eye. The very simple and effective strategy reported here facilitates the development of portable and reliable fluorescence nanosensors for the determination of Hg^{2+} in real samples.



Heavy metal contamination widely lies in water, air, soil, or foods and thus has remained a serious concern across the world for decades. In particular, mercury with a very high toxicity can lead to a variety of permanent damages to human health even at a very low concentration,¹ and people are thus put on high alert to avoid the occurrence of shocking pollutant events. Therefore, the detection of mercury ions is a necessary thing to be done by governments or societal institutions, which plays a crucial role in environmental protection and food safety. The mercury ions assays are usually performed by a wealth of established techniques including cold-vapor atomic fluorescence spectrometry,² cold-vapor atomic absorption spectrometry,³ inductively coupled plasma-mass spectrometry,⁴ and X-ray absorption spectroscopy.⁵ Although these methods could fully meet the demands of sensitivity and selectivity in the assays of mercury ions, they are usually expensive and time-consuming and require tedious sample pretreatments and enrichments, sophisticated instrumentations, and personnel training. Therefore, it still remains a challenge to achieve sensitive but simple, rapid, and inexpensive detection to mercury ions.

Toward this goal, considerable efforts have been contributed to the development of chemosensors to the simple and on-site detection of Hg^{2+} via cooperative recognition and signaling, in particular, the employment of optical materials such as organic dyes^{6–9} and functionalized nanomaterials.^{10–17} Different dye derivatives have been reported to selectively bind with Hg^{2+} for fluorescent assays, and various nanomaterials such as luminescent quantum dots,¹⁵ plasmonic metal nanoparticles,¹⁶ and upconversion nanoparticles¹⁷ have also been demonstrated to probe Hg^{2+} by the modification with ligands at their surfaces using the optical readout. However, most of these sensors are based on fluorescence quenching in the presence of Hg^{2+} , which have to suffer from the multiple interferences caused by external quenchers or other environmental factors in practical applications. It has been widely recognized that fluorescence enhancement (“turn on”) is preferable to fluorescence quenching (“turn off”) because of higher target selectivity and less false positives.

Received: September 11, 2013

Accepted: December 30, 2013

Published: December 30, 2013

The newly emerging fluorescence carbon nanodots (CDs), due to their low cytotoxicity, good water solubility, chemical inertness, easy preparation, and environmental friendliness, have attracted extensive research interest since their discovery by Scrivens and co-workers in 2004.¹⁸ In the past few years, much effort has been contributed to the synthesis and property of CDs¹⁹ and their application in bioimaging,²⁰ photocatalysis,²¹ and optoelectronic devices.²² Recently, the chemosensors with the use of fluorescent CDs for the detection of biomolecules²³ and metal ions^{24,25} have been also reported based on the quenching mechanism of CDs fluorescence. In the case of metal ions, however, many heavy metal ions can quench the fluorescence of CDs through an effective electron or energy transfer process,²⁴ leading to a very bad selectivity for specific metal ions. In contrary, the fluorescence “turn on” by the surface-functionalized design of CDs may be a conceivable strategy to overcome the problems toward the selective detection of heavy metal ions.

In the present work, we reported for the first time the use of a bis(dithiocarbamato)copper(II) complex functionalized CDs (CuDTC₂-CDs) for the fluorescence “turn on” detection of Hg²⁺ with high sensitivity and selectivity. Amine-coated CDs was selected as the fluorescence nanomaterial based on the fact that amine group could readily react with carbon disulfide to form dithiocarbamates, which could promptly form complexes with Cu²⁺, facilitating the further functionalization of the CDs with CuDTC₂ complex through a layer-by-layer procedure. The CuDTC₂-CDs probe initially showed very weak fluorescence because of the quenching effect of the surface bound CuDTC₂ through a combination of electron transfer and energy transfer mechanism. Because of the stronger chelating ability of Hg²⁺ to dithiocarbamates than that of Cu²⁺, the structure of the surface bound CuDTC₂ complex could be readily transformed into more stable HgDTC₂ in the presence of Hg²⁺, leading to the shutdown of the energy transfer pathway and thus the fluorescence enhancement of the CDs probe solution immediately. Moreover, a portable paper-based sensor has been developed by printing the CuDTC₂-CDs probe solution on cellulose acetate papers using a commercial inkjet printer. Visual fluorescence detection of Hg²⁺ with the naked eye was achieved under a UV lamp, suggesting its potential in practical application for the detection of Hg²⁺.

■ EXPERIMENTAL SECTION

Materials. 4,7,10-Trioxa-1,13-tridecanediamine (TTDDA) and glycerol were purchased from Sigma-Aldrich. Carbon disulfide (99%), sarcosine, citric acid, chloroauric acid tetrahydrate, and all the metal salts were obtained from Sinopharm Chemical Reagent and used without further purification. Ultrapure water (18 MΩ) was used for the preparation of all solutions.

Synthesis of Amine-Coated Carbon Nanodots (CDs). Amine-coated carbon nanodots (CDs) were synthesized by pyrolyzing the mixture of citric acid and TTDDA in glycerol according to the reported method with minor modification.²⁶ Briefly, 1 g of TTDDA was added into 15 mL of glycerol to form a clear solution, and the resulting solution was heated to 220 °C under nitrogen atmosphere. Then, 1 g of citric acid was quickly added into the hot solution and the temperature was kept at 220 °C for another 3 h. A dark brown solution was obtained and cooled down to room temperature naturally. After the dialysis through a membrane with molecular weight cutoff of approximately 3500 for 48 h, a purified amine-coated carbon

nanodots solution was collected and kept in the dark for future use.

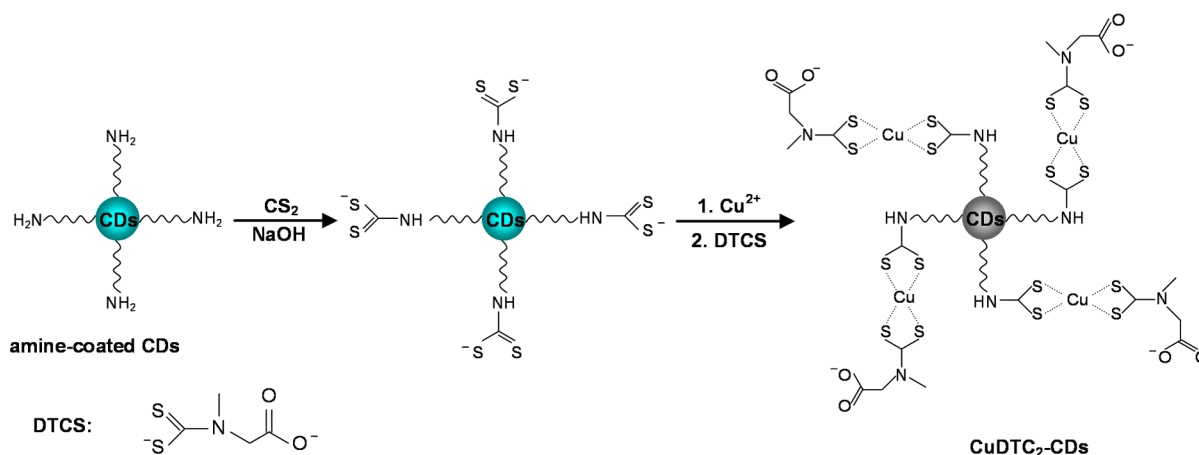
Synthesis of Ammonium *N*-(dithiocarbonyl) Sarcosine (DTCS) and Cu(DTCS)₂ Complex. Ammonium *N*-(dithiocarbonyl) sarcosine (DTCS) was synthesized according to the reported method.²⁷ Briefly, 5.02 g of sarcosine (56.1 mmol) was dissolved in 15 mL of aqueous ammonia (25%) under stirring in an ice bath. Then, the mixture of 5.6 mL of carbon disulfide and 15 mL of absolute ethanol was added dropwise into the above ice-cold sarcosine solution under vigorous stirring with the addition rate of about 20 mL/h. The above mixture was stirred for another 12 h at room temperature, and meanwhile white DTCS-NH₄ solid precipitated from the solution. The precipitate was washed sequentially with ice methanol and dry ether. The product was further purified by the recrystallization with methanol. The Cu(DTCS)₂ complex was synthesized by mixing CuCl₂ and DTCS in water at the molar ratio of 1 to 2.

Preparation of Bis(dithiocarbamato)copper(II) Complex Functionalized Carbon Nanodots (CuDTC₂-CDs). Briefly, 1 mL of the as-prepared amine-coated CDs and 200 μL of sodium hydroxide (1 M) were added into 3 mL of ethanol to form a homogeneous solution and kept in an ice bath. A volume of 200 μL of carbon disulfide (dissolved in 1 mL of absolute ethanol) was then added dropwise into the above solution under vigorous stirring in an ice bath. After reaction for 5 h, 5 mL of diethyl ether anhydrous was added into the above system and vigorously stirred for 1 min prior to centrifugation at 5000 rpm for 10 min. The obtained precipitate was dissolved in 2 mL of water to form a clear solution. A volume of 1 mL of aqueous Cu²⁺ (10 mM) was then added into the solution, and the resulting turbid solution was centrifuged and the precipitate was collected. A volume of 200 μL of DTCS (10 mM) was added into the above precipitate to form a clear brown solution. The purified bis(dithiocarbamato)copper(II) complex functionalized carbon nanodots (CuDTC₂-CDs) solution was finally obtained by the dialysis for 48 h.

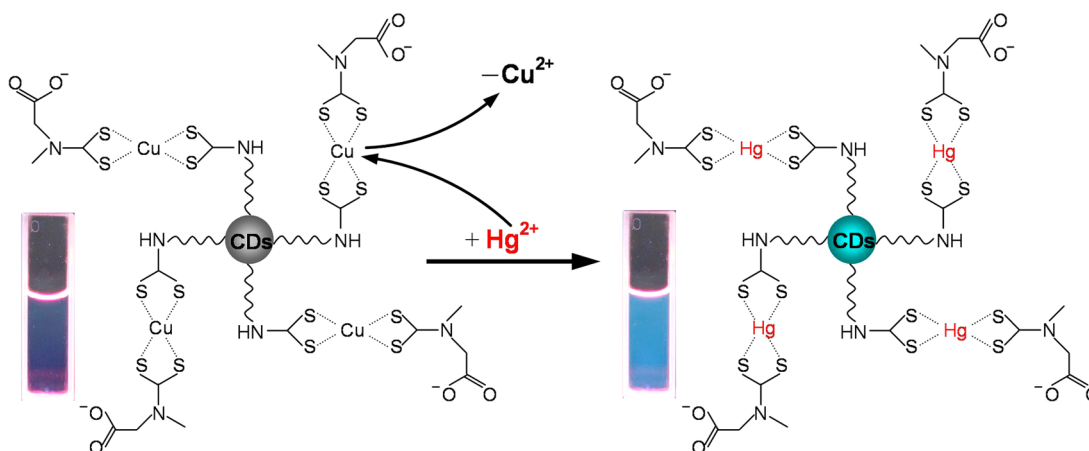
Fluorescence Response of the CuDTC₂-CDs Probe to Hg²⁺. In brief, 200 μL of the bis(dithiocarbamato)copper(II) complex functionalized carbon nanodots (CuDTC₂-CDs) solution was added into 1.8 mL of water in a spectrophotometer quartz cuvette to form the probe solution. Then 2 μL of a known concentration of Hg²⁺ stock solution was injected into the above probe solution and mixed thoroughly by the pipettor to form a homogeneous mixture. The fluorescence spectra were recorded using 365 nm excitation wavelength. All the fluorescence intensities were an average of three independent measurements. For comparison, the fluorescence response of the CuDTC₂-CDs to other metal ions was also performed by the same method.

Preparation of Paper-Based Sensor for Visual Detection of Hg²⁺. A common cartridge of a commercial inkjet printer was washed with ultrapure water until the ink powder was cleared away completely followed by drying in an oven at 50 °C for 6 h. The empty cartridge was loaded with the CuDTC₂-CDs aqueous solution as the printing ink. The probe solution was then printed on a piece of cellulose acetate microporous membrane by an inkjet printer connected to a computer to obtain Hg²⁺-responsive paper sensors. For the visual detection of Hg²⁺, 10 μL of Hg²⁺ aqueous solution with different concentrations was carefully dropped onto the printed pattern and air-dried for 10 min. The fluorescence color

Scheme 1. Schematic Illustration for the Preparation of Bis(dithiocarbamato)copper(II) Complex Functionalized Carbon Nanodots (CuDTC₂-CDs) Probe



Scheme 2. Schematic Illustration for the Fluorescent “Turn On” Nanosensor to Detect Hg²⁺ by the Hg²⁺-Induced Displacement of Cu²⁺ in the Surface Bound CuDTC₂ Complex



responses of the indicating paper were observed under a portable UV lamp with the excitation wavelength of 365 nm.

Instrumentation. UV–vis absorption and fluorescence spectra were recorded with a Shimadzu UV-2550 spectrometer and Pekin-Elmer LS-55 luminescence spectrometer, respectively. Photographs were taken with a Canon 600D digital camera. The sizes and morphologies of the CDs were observed using a JEOL 2010 transmission electron microscope. Fourier transform infrared (FT-IR) spectra were recorded on a Thermo Fisher Nicolet iS10 FT-IR spectrometer.

RESULTS AND DISCUSSION

Amine-Coated CDs and CuDTC₂-CDs. The CDs were prepared by heating citric acid in glycerol at 220 °C under nitrogen in the presence of a surface coating agent 4,7,10-trioxa-1,13-tridecanediamine, resulting in the existence of amine groups on the surface of CDs. As revealed by the TEM image (Figure S1a in the Supporting Information), the as-prepared amine-coated CDs possessed good monodispersity with the diameter of about 10 nm. Moreover, the aqueous CDs solution exhibited the excitation-wavelength-dependent emission spectra and gave out bright-blue fluorescence under the excitation of 365 nm (Figure S1b in the Supporting Information).

It is widely recognized that carbon disulfide could readily react with primary or secondary amines to form dithiocarba-

mates compounds, which exhibits a strong chelating ability to heavy metal ions and is thus extensively used for the functionalization of noble metal nanoparticles and semiconductor quantum dots.^{28,29} With this approach, bis-(dithiocarbamato)copper(II) complex (CuDTC₂) was conjugated to the surface of the CDs through a layer-by-layer procedure (Scheme 1). Initially, the amine groups on the surface of the CDs were treated with carbon disulfide and sodium hydroxide to form dithiocarbamate groups (DTC), followed by the coordination of copper(II) to the resulting DTC groups.³⁰ Because of the fact that the bidentate ligand dithiocarbamate promptly forms complexes with many transition metals,³¹ the coordination between copper(II) and the DTC group on the surface of the CDs could be readily accomplished by simply mixing them in aqueous solution. Finally, dithiocarbamate salt (ammonium *N*-(dithiocarbamoyl)sarcosine, DTCS) was added to further coordinate with the Cu²⁺ to form the double-ligand complex CuDTC₂ at the surface of CDs. Because of the carboxyl group in the DTCS molecule, the CuDTC₂-CDs were readily dispersed in water and retained its good monodispersity (see the TEM image of Figure S2 in the Supporting Information), in which no aggregate was observed at room temperature for at least 6 months (Figure S3 in the Supporting Information). The conjugation of CuDTC₂ complex at the surface of CDs was examined by infrared (IR)

spectroscopy. As shown in Figure S4 in the Supporting Information, the bands at 3430 cm^{-1} and 1100 cm^{-1} were assigned to the N–H and C–N vibrations, respectively, confirming the presence of NH_2 on the surface of the CDs.³² The strong vibration bands at 1594 cm^{-1} and 1400 cm^{-1} were ascribed to the asymmetric and symmetric stretch of the COO^- group, respectively.³² Moreover, the bands at 1530 cm^{-1} and 618 cm^{-1} were assigned to the C–N stretch and C–S symmetric stretch of $\text{S}_2\text{C-NHR}$ in the dithiocarbamate group, respectively.^{32–34} These indicate that the CuDTC_2 complex has been successfully conjugated onto the surface of the CDs.

Mechanism of the CuDTC_2 -CDs Fluorescence Nano-sensor for Hg^{2+} Detection. Scheme 2 illustrates the fluorescence “turn on” mechanism for the detection of Hg^{2+} using the CuDTC_2 -CDs. The CuDTC_2 -CDs probe showed very weak fluorescence with the relative fluorescence intensity of about 16% as compared to the initial amine-coated CDs (Figure S5 in the Supporting Information). Since the transition metal copper possesses half-filled energy levels (d orbitals) available for the exchange of electrons with the photoexcited CDs, the fluorescence quenching probably originated by the electron transfer between Cu^{2+} and CDs to facilitate the nonradiative recombination.^{35,36} Moreover, the energy transfer caused by the surface bound CuDTC_2 complex may also be another mechanism for the fluorescence quenching of the CuDTC_2 -CDs, which could be explained by the absorption spectrum of the CuDTC_2 complex and the emission spectrum of the CDs. Figure 1 shows that the CuDTC_2 complex has a

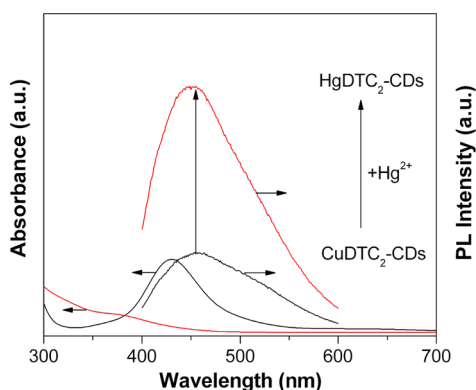


Figure 1. UV–vis absorption spectra of the $\text{Cu}(\text{DTCS})_2$ before (black line) and after (red line) the addition of Hg^{2+} , and the fluorescence spectra of CuDTC_2 -CDs probe before (black line) and after (red line) the addition of Hg^{2+} at an excitation wavelength of 365 nm .

wide absorption with the peak at 432 nm , partially overlapping with the emission peak of the CDs at 450 nm . Therefore, the energy transfer from the excited CDs to the surface bound CuDTC_2 complex can result in the fluorescence quenching of the CuDTC_2 -CDs probe. Upon the addition of Hg^{2+} into the probe solution, the displacement of Cu^{2+} by Hg^{2+} in the complex forms more stable HgDTC_2 complex because the mercury dithiocarbamates has a much higher equilibrium constant than copper dithiocarbamates.³⁷ The reaction leads to the disappearance of absorption at 432 nm and thus shuts off the pathway of energy transfer. Accordingly, the fluorescence of CDs can be recovered in the presence of Hg^{2+} , as shown in Figure 1.

To better understand the interaction between Hg^{2+} and CuDTC_2 complex in aqueous solution, the coordination state

between Cu^{2+} and DTCS was first investigated through the titration experiments. Figure 2A shows the absorption spectra changes of the titration of DTCS solution with Cu^{2+} . The free DTCS aqueous solution exhibits two characteristic absorption bands at 256 and 283 nm , whereas its complex with Cu^{2+} also had two characteristic absorption peaks, which were dependent on their molar ratio in solution. At the molar ratio range from $0.05:1$ ($\text{Cu}^{2+}/\text{DTCS}$) to $0.5:1$, their coordination complex showed two characteristic bands at 432 and 268 nm with a brownish-yellow color in natural light and reached its maximum at the molar ratio of $0.5:1$ (the top set spectra in Figure 2A), indicating the coordination between Cu^{2+} and DTCS was bis-complex state ($\text{Cu}(\text{DTCS})_2$), which was consistent with the feature of analogous CuDTC_2 complexes in the literature.³⁷ However, upon the increase addition of Cu^{2+} , both of the two bands at 432 and 268 nm gradually shifted to 385 and 261 nm , respectively, and reached its maximum at the molar ratio of $1:1$, accompanied with the color change from brownish-yellow to light green, implying the complete transition of bis-complex to monocomplex state (CuDTCS), which could be evidenced by the appearance of an isosbestic point at 400 nm upon the addition of Cu^{2+} (the bottom set spectra in Figure 2A). Moreover, the result obtained from the titration of Cu^{2+} solution by DTCS showed that the monocomplex CuDTCS could also transfer to bis-complex ($\text{Cu}(\text{DTCS})_2$) by simply increasing the molar ratio ($\text{DTCS}:\text{Cu}^{2+}$) to $2:1$ from $1:1$ (Figure 2B). Therefore, it is concluded that there were two complex states (mono- and bis-complex) between Cu^{2+} and DTCS, which were dependent on their molar ratios and could be easily discriminated by the characteristic absorption bands and the colors of their solution.

Figure 2C shows the evolution of absorption spectra of $\text{Cu}(\text{DTCS})_2$ solution upon the addition of Hg^{2+} . The characteristic bands of $\text{Cu}(\text{DTCS})_2$ at 268 and 432 nm were gradually shifted to 261 and 385 nm , respectively, and reached its maximum at the molar ratio of $0.5:1$ ($\text{Hg}^{2+}/\text{Cu}(\text{DTCS})_2$), accompanied with the solution color change from brownish-yellow to light green (the top set spectra in Figure 2C). Moreover, an isosbestic point at 394 nm can be clearly seen upon the increasing addition of Hg^{2+} , which definitely evidenced the complete transition of $\text{Cu}(\text{DTCS})_2$ to CuDTCS . Furthermore, it is observed that the monocomplex CuDTCS started to be broken upon the further increase of Hg^{2+} concentration, according to the gradual disappearance of its characteristic bands at 261 and 385 nm and the color change of the solution from light green to colorless at the molar ratio of $0.55:1$ ($\text{Hg}^{2+}/\text{Cu}(\text{DTCS})_2$) to $1:1$ (the bottom set spectra in Figure 2C). Moreover, another isosbestic point at 373 nm can be clearly seen, indicating the complete displacement of Cu^{2+} in the CuDTCS complex by Hg^{2+} in a 2 -to- 1 stoichiometric reaction. These results suggested that the CuDTC_2 complex on the surface of the CDs could be readily transformed into a more stable HgDTC_2 complex.

Fluorescence Detection of Hg^{2+} Using the CuDTC_2 -CDs Probes. The fluorescence response time of the CuDTC_2 -CDs probe to Hg^{2+} was first investigated prior to the sensitivity study. The result showed that the fluorescence of the probe was enhanced by about 60% in 1 min after the addition of Hg^{2+} (80 nM) and remained unchanged with a further increase of reaction time, indicating that it was very fast to reach an equilibrium in the interaction between Hg^{2+} and the probe (Figure S6 in the Supporting Information). Figure 3A shows the evolution of fluorescence spectra after adding $2\text{ }\mu\text{L}$ of

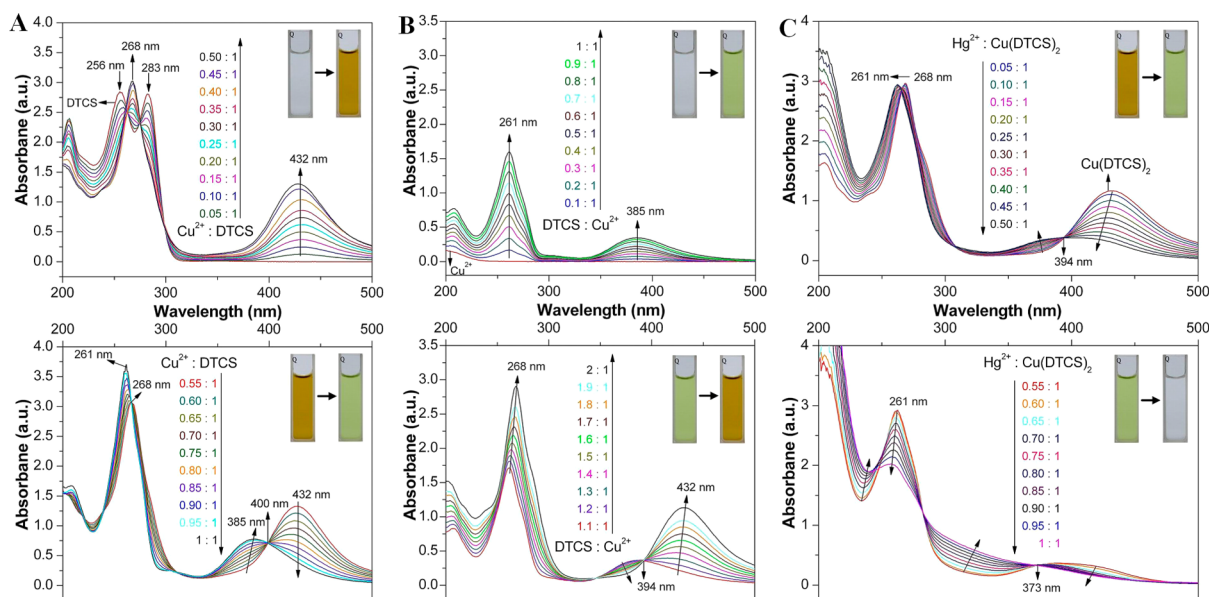


Figure 2. UV-vis absorption spectra responses of (A) DTCS aqueous solution (2 mM) upon the addition of Cu^{2+} at the molar ratio ($\text{Cu}^{2+}/\text{DTCS}$) ranges from 0.05:1 to 0.5:1 (top) and 0.55:1 to 1:1 (bottom), (B) Cu^{2+} aqueous solution (1 mM) upon the addition of DTCS at the molar ratio ($\text{DTCS}/\text{Cu}^{2+}$) ranges from 0.1:1 to 1:1 (top) and 1:1 to 2:1 (bottom), and (C) $\text{Cu}(\text{DTCS})_2$ aqueous solution (1 mM) upon the addition of Hg^{2+} at the molar ratio ($\text{Hg}^{2+}/\text{Cu}(\text{DTCS})_2$) ranges from 0.05:1 to 0.5:1 (top) and 0.55:1 to 1:1 (bottom). The inset images are the corresponding color changes of the solution under natural light.

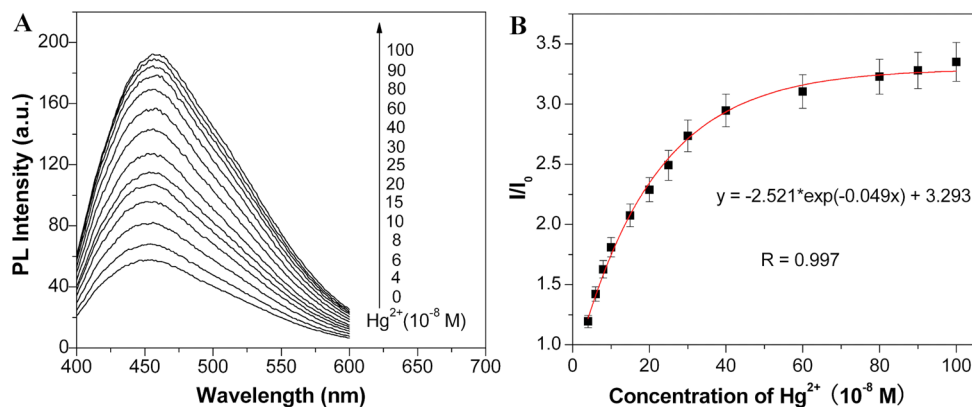


Figure 3. (A) Fluorescence enhancement of the $\text{CuDTCS}_2\text{-CDs}$ probe solution (10 $\mu\text{g/mL}$) with the addition of Hg^{2+} . (B) Plot of fluorescence enhancement as a function of the Hg^{2+} concentrations. I_0 and I are the fluorescence intensity of the $\text{CuDTCS}_2\text{-CDs}$ probe solution in the absence and in the presence of Hg^{2+} , respectively.

aqueous Hg^{2+} into the $\text{CuDTCS}_2\text{-CDs}$ probe solution. With the increase of Hg^{2+} concentration from 40 nM to 1 μM , the fluorescence of the CDs gradually enhanced and finally reached to about 3.4-fold stronger than that of the initial probe solution. Even at the concentration of 40 nM, the fluorescence was still enhanced by 18%, demonstrating a sensitive response to Hg^{2+} by the $\text{CuDTCS}_2\text{-CDs}$ probe. Figure 3B shows the plot of fluorescence enhancement (I/I_0) against the concentration of Hg^{2+} . The fitted curve could be used for the quantification of Hg^{2+} with a correlation coefficient of 0.997, and the detection limit could reach as low as 20 nM (4 ppb) based on the definition of 3 times the deviation of the blank signal (3σ).

The selectivity of detection of Hg^{2+} was further examined by the addition of other metal ions into the probe solution. Figure 4A shows that the additions of K^+ , Na^+ , Ca^{2+} , Cd^{2+} , Mg^{2+} , Zn^{2+} , Fe^{3+} , Ba^{2+} , Cu^{2+} , Pb^{2+} , Ni^{2+} , and Co^{2+} cannot cause any significant fluorescence enhancement. The selectivity of fluorescence enhancement to Hg^{2+} was remarkably higher

than to these metal ions, in which the fluorescence intensity of the $\text{CuDTCS}_2\text{-CDs}$ probe solution was enhanced by about 3-fold and 2.5-fold at the concentrations of 600 nM and 250 nM, respectively (Figure 4B). In addition, the interference experiments were also carried out by comparing the fluorescence enhancement of the probe solution in the presence of these metal ions at relative high concentration (Figure S7 in the Supporting Information). The fluorescence enhancement of the probe solution by the addition of Hg^{2+} was not influenced by the coexistence of other metal ions tested. One of main reason is that these metal ions have a much poorer chelating ability with dithiocarbamates than Hg^{2+} and thus cannot replace the Cu^{2+} in the complex.³⁷

It should be noted that the addition of Ag^+ and AuCl_4^- can also slightly enhance the fluorescence of the $\text{CuDTCS}_2\text{-CDs}$ probe solution and thus may bring interferences for the detection of Hg^{2+} in real water samples (Figure S8a in the Supporting Information). Fortunately, the interference caused

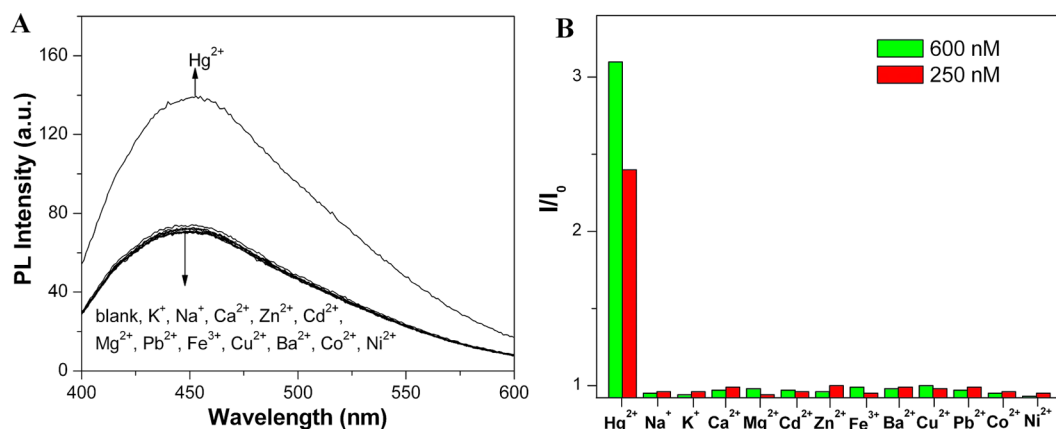


Figure 4. (A) Fluorescence responses of the CuDTC₂-CDs probe solution (10 µg/mL) in the presence of various metal ions. The concentrations of all metal ions are 150 nM. (B) The fluorescence enhancement (I/I_0) of CuDTC₂-CDs probe after the addition of metal ions at 250 nM and 600 nM, respectively. I_0 and I represent the fluorescence intensity of the CuDTC₂-CDs probe solution in the absence and in the presence of metal ions, respectively.

Table 1. Application of the CuDTC₂-CDs Probes to the Determination of Hg²⁺ in Tap Water, Local Lake Water, and Human Urine Samples^a

spiked concentration/nM	tap water		lake water		urine sample	
	found/nM	recovery (%)	found/nM	recovery (%)	found/nM	recovery (%)
80	84.3	105 ± 2.8	76.1	95.1 ± 3.7	91.0	113.7 ± 2.6
200	192.7	96.4 ± 1.4	209.5	104.8 ± 2.1	224.3	112.2 ± 3.1
400	415.2	103.8 ± 2.5	411.4	102.9 ± 2.9	426.8	106.7 ± 2.3

^aValues shown were the calculated mean Hg²⁺ concentration for each sample and were determined from three replicates.

by AuCl₄[−] could be ignored because it is generally not present in water system due to its highly oxidizing ability. As for Ag⁺, its interference can be easily suppressed by a simple sample pretreatment with chloride ion because Ag⁺ can promptly form insoluble AgCl with Cl[−]. After the simple pretreatment, the fluorescence responses of the CuDTC₂-CDs probe to the single Hg²⁺ solution and to the pretreated mixture solution of Hg²⁺ and Ag⁺ were nearly the same (Figure S8b in the Supporting Information).

Practical Application in Environmental Water Samples. To assess the utility of the Hg²⁺-responsive CuDTC₂-CDs probes, the determination of Hg²⁺ in environmental water samples including tap water, local lake water (Shushan Lake), and human urine sample has been tested. All the samples were filtered through 0.45 µm Supor filters to remove any particulate suspension prior to the preparation of samples by spiking the original samples with known amounts of Hg²⁺ at three different concentrations (80, 200, and 400 nM). It is noted that there was no detectable Hg²⁺ existing in all the three original samples according to the inductively coupled plasma mass spectrometry (ICPMS) method. Each measurement was done in triplicate, and the average was presented with standard deviation. The results summarized in Table 1 shows good agreement between experimental and actual values for Hg²⁺ concentrations in tap water and local lake water, indicating the utility of the proposed CuDTC₂-CDs-based nanosensors. However, the recoveries for human urine sample are much higher than 100% (113.7%, 112.2%, and 106.7%), indicating its positive interference for the determination of Hg²⁺. This could be ascribed to the complicated biomolecules in a human urine sample, which could also exhibit weak fluorescence under the excitation of UV-light (background autofluorescence). Therefore, all the results summarized in Table 1 are satisfying and reasonable,

suggesting that the CuDTC₂-CDs-based fluorescence probes for Hg²⁺ detection are reliable and possess the potential in practical applications.

Paper-Based Sensor for Visual Fluorescence Detection of Hg²⁺. To develop a simple, cheap, portable, and reliable paper-based sensor is the ultimate goal for the instant on-site detection in practical applications. Recently, fluorescence nanomaterials (semiconductor quantum dots, fluorescence graphene oxide) have exhibited the potentials to prepare paper-based nanosensors for the visual fluorescent detection of some analytes such as trinitrotoluene and biomolecules.^{38–40} Here, a Hg²⁺-responsive paper sensor has been developed for the visual fluorescence detection of aqueous Hg²⁺ by printing the CuDTC₂-CDs probe solution on a piece of cellulose acetate microporous membrane with a pore size of 0.45 µm, followed by air-drying for 5 min. The printed pattern “Mercury(II)” almost could not be seen under natural light (the left image in Figure 5). However, after dropping 10 µL of aqueous Hg²⁺ solution onto the printed pattern and air-drying for 10 min, the fluorescence of the printed pattern gradually appeared along with the increase of Hg²⁺ concentration under a UV lamp (the right image in Figure 5). At the Hg²⁺ concentration of 10 µM, an obvious fluorescence enhancement of the printed pattern could be clearly observed. Even at 0.4 µM of Hg²⁺, the fluorescence of “Mercury(II)” can still be distinguished under a UV lamp with the naked eye. Although the accurate quantitative assay using a digital camera has not still been achieved in this work, this change of fluorescence brightness on the paper can also indicate roughly the range of Hg²⁺ concentrations. Significantly, the paper sensor is much simpler and more convenient for the determination of Hg²⁺ than these reported methods.

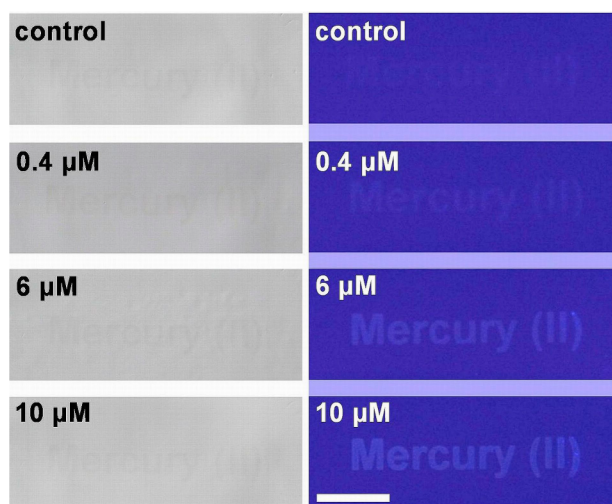


Figure 5. Paper-based visual detection of aqueous Hg^{2+} at three concentrations of 0.4, 6, and 10 μM . The images on the left are taken under natural light. The corresponding fluorescence images under the 365 nm UV lamp are shown on the right. The scale bar is 1 cm.

CONCLUSIONS

In summary, we have developed a novel fluorescence “turn on” sensor for the determination of aqueous Hg^{2+} with high sensitivity and selectivity using CuDTC_2 -CDs. It has been demonstrated that the fluorescence of the CDs is quenched by the CuDTC_2 complex bound to its surface through a combination of electron transfer and energy transfer mechanism, and Hg^{2+} can readily replace the Cu^{2+} to form a more stable HgDTC_2 complex, resulting in the fluorescence “turn on” of the CDs by shutting off the energy transfer pathway. The fluorescence “turn on” by the complexing displacement reaction significantly improves the selectivity of detection of Hg^{2+} and thus decreases the interference of other metal ions at the largest degree. The results from the recovery experiments suggest its applicability for the analysis of Hg^{2+} in real environmental water samples. Moreover, a paper-based sensor has been developed by simply printing the CuDTC_2 -CDs probe solution on the cellulose acetate papers for the instant, on-site, and visual detection of Hg^{2+} in practical application. In particular, the CDs-based nanosensor is very simple, rapid, inexpensive, and environmentally friendly. The strategy reported here will open a novel pathway to the detection of metal ions by the design of surface coordination chemistry on the functional nanomaterials.

ASSOCIATED CONTENT

Supporting Information

Additional information as noted in text. This material is available free of charge via the Internet at <http://pubs.acs.org>.

AUTHOR INFORMATION

Corresponding Authors

*E-mail: bhliu@iim.ac.cn.

*E-mail: zpzhang@iim.ac.cn.

Notes

The authors declare no competing financial interest.

ACKNOWLEDGMENTS

This work was supported by the National Key Technology R&D Program (Grant 2012BAJ24B02), the Technology Planning Project of Fujian Province (Grant No. 2013Y0031), and the Natural Science Foundation of China (Grant Nos. 21275145, 21375131, and 21175137).

REFERENCES

- (1) Nolan, E. M.; Lippard, S. J. *Chem. Rev.* **2008**, *108*, 3443–3480.
- (2) Clevenger, W. L.; Smith, B. W.; Winefordner, J. D. *Crit. Rev. Anal. Chem.* **1997**, *27*, 1–26.
- (3) Kunkel, R.; Manahan, S. E. *Anal. Chem.* **1973**, *45*, 1465–1468.
- (4) Bings, N. H.; Bogaerts, A.; Broekaert, J. A. C. *Anal. Chem.* **2006**, *78*, 3917–3946.
- (5) Bernaus, A.; Gaona, X.; Esbrí, J. M.; Higuera, P.; Falkenberg, G.; Valiente, M. *Environ. Sci. Technol.* **2006**, *40*, 4090–4095.
- (6) Aragay, G.; Pons, J.; Merkoçi, A. *Chem. Rev.* **2011**, *111*, 3433–3458.
- (7) Aragay, G.; Montón, H.; Pons, J.; Font-Bardía, M.; Merkoçi, A. *J. Mater. Chem.* **2012**, *22*, 5978–5983.
- (8) Aragay, G.; Alarcón, G.; Pons, J.; Font-Bardía, M.; Merkoçi, A. *J. Phys. Chem. C* **2012**, *116*, 1987–1994.
- (9) Wegner, S. V.; Okesli, A.; Chen, P.; He, C. *J. Am. Chem. Soc.* **2007**, *129*, 3474–3475.
- (10) Zhang, L.; Chang, H. X.; Hirata, A.; Wu, H. K.; Xue, Q. K.; Chen, M. W. *ACS Nano* **2013**, *7*, 4595–4600.
- (11) Aragay, G.; Pons, J.; Ros, J.; Merkoçi, A. *Langmuir* **2010**, *26*, 10165–10170.
- (12) Liu, D. B.; Qu, Q. S.; Chen, W. W.; Zhang, W.; Wang, Z.; Jiang, X. Y. *Anal. Chem.* **2010**, *82*, 9606–9610.
- (13) Deng, L.; Ouyang, X. Y.; Jin, J. Y.; Ma, C.; Jiang, Y.; Zheng, J.; Li, J. S.; Li, Y. H.; Tan, W. H.; Yang, R. H. *Anal. Chem.* **2013**, *85*, 8594–8600.
- (14) Placido, T.; Aragay, G.; Pons, J.; Comparelli, R.; Curri, M. L.; Merkoçi, A. *ACS Appl. Mater. Interfaces* **2013**, *5*, 1084–1092.
- (15) Freeman, R.; Finder, T.; Willner, I. *Angew. Chem., Int. Ed.* **2009**, *48*, 7818–7821.
- (16) Huang, C.; Yang, Z.; Lee, K.; Chang, H. *Angew. Chem., Int. Ed.* **2007**, *46*, 6824–6828.
- (17) Liu, Q.; Peng, J. J.; Sun, L. N.; Li, F. Y. *ACS Nano* **2013**, *5*, 8040–8048.
- (18) Xu, X. Y.; Ray, R.; Gu, Y. L.; Ploehn, H. J.; Gearheart, L.; Raker, K.; Scrivens, W. A. *J. Am. Chem. Soc.* **2004**, *126*, 12736–12737.
- (19) Baker, S. N.; Baker, J. A. *Angew. Chem., Int. Ed.* **2010**, *49*, 6726–6744.
- (20) Yu, S. J.; Kang, M. W.; Chang, H. C.; Chen, K. M.; Yu, Y. C. *J. Am. Chem. Soc.* **2005**, *127*, 17604–17605.
- (21) Li, H. T.; He, X. D.; Kang, Z. H.; Huang, H.; Liu, Y.; Liu, J. L.; Lian, S. Y.; Tsang, C. H. A.; Yang, X. B.; Lee, S. T. *Angew. Chem., Int. Ed.* **2010**, *49*, 4430–4434.
- (22) Yan, X.; Cui, X.; Li, B.; Li, L. *Nano Lett.* **2010**, *10*, 1869–1873.
- (23) Yu, C. M.; Li, X. Z.; Zeng, F.; Zheng, F. Y.; Wu, S. Z. *Chem. Commun.* **2013**, *49*, 403–405.
- (24) Dong, Y. Q.; Wang, R. X.; Li, G. L.; Chen, C. Q.; Chi, Y. W.; Chen, G. N. *Anal. Chem.* **2012**, *84*, 6220–6224.
- (25) Zhu, A. W.; Qu, Q.; Shao, X. L.; Kong, B.; Tian, Y. *Angew. Chem., Int. Ed.* **2012**, *51*, 7185–7189.
- (26) Shi, W.; Li, X. H.; Ma, H. M. *Angew. Chem., Int. Ed.* **2012**, *51*, 6432–6435.
- (27) Wang, S. H.; Han, M. Y.; Huang, D. J. *J. Am. Chem. Soc.* **2009**, *131*, 11692–11694.
- (28) Dubois, F.; Mahler, B.; Dubertret, B.; Doris, E.; Mioskowski, C. *J. Am. Chem. Soc.* **2007**, *129*, 482–483.
- (29) Zhao, Y.; Pérez-Segarra, W.; Shi, Q. C.; Wei, A. *J. Am. Chem. Soc.* **2005**, *127*, 7328–7329.
- (30) Cao, R.; Diaz, A.; Cao, R.; Otero, A.; Cea, R.; Rodríguez-Argüelles, M. C.; Serra, C. *J. Am. Chem. Soc.* **2007**, *129*, 6927–6930.

- (31) Yan, Y.; Krishnakumar, S.; Yu, H.; Ramishetti, S.; Deng, L. W.; Wang, S. H.; Huang, L.; Huang, D. J. *J. Am. Chem. Soc.* **2013**, *135*, 5312–5315.
- (32) Thirumaran, S.; Ramalingam, K. *Trans. Metal Chem.* **2000**, *25*, 60–62.
- (33) Macias, B.; Villa, M. V.; Martin-Simon, M. *Trans. Metal Chem.* **1999**, *24*, 533–536.
- (34) Geetha, N.; Thirumaran, S. *J. Serb. Chem. Soc.* **2008**, *73*, 169–177.
- (35) Chen, Y.; Rosenzweig, Z. *Anal. Chem.* **2002**, *74*, 5132–5138.
- (36) Ruedas-Rama, M. J.; Hall, E. A. H. *Anal. Chem.* **2008**, *80*, 8260–8268.
- (37) Fritz, J. S.; Sutton, S. A. *Anal. Chem.* **1956**, *28*, 1300–1303.
- (38) Yuan, C.; Zhang, K.; Zhang, Z. P.; Wang, S. H. *Anal. Chem.* **2012**, *84*, 9792–9801.
- (39) Zhang, K.; Zhou, H. B.; Mei, Q. S.; Wang, S. H.; Guan, G. J.; Liu, R. Y.; Zhang, J.; Zhang, Z. P. *J. Am. Chem. Soc.* **2011**, *133*, 8424–8427.
- (40) Mei, Q. S.; Zhang, Z. P. *Angew. Chem., Int. Ed.* **2012**, *51*, 5602–5606.